Neuron, Volume 60

Supplemental Data

Destabilization of the Postsynaptic Density by PSD-95 Serine 73 Phosphorylation Inhibits Spine Growth and Synaptic Plasticity

Pascal Steiner, Michael J. Higley, Weifeng Xu, Brian L. Czervionke, Robert C. Malenka and Bernardo L. Sabatini

Supplemental Material and Methods

DNA constructs and evaluation of expression levels

All enzymes were obtained from New England Biolabs. The plasmids containing the following cDNAs were gifts: pdsRed-T1-N1 (B. Glick, University of Chicago, Chicago, IL, USA), pPAGFP-N1/C1 (G. Patterson, NICHD, Bethesda, MD), pPSD-95-CFP-N1 (M. Sheng, MIT, Cambridge, MA, USA), pPSD-95 ΔGK-GFP-GW1 and pPSD-95 ΔPDZ1,2-GFP-GW1 (R.A. Nicoll, University of California, San Francisco, CA, USA), shPSD-95-FUGW (R. C. Malenka, Stanford University, CA, USA), GFP-SHANK2 (S. Okabe, Medical and Dental University, Tokyo, Japan). For the generation of PSD-95-GFP and PSD-95-PAGFP,, the CFP was replaced by PCR-amplified GFP or PAGFP in frame at the sites SacII/NotI. The deletion mutant of PSD-95, ΔPDZ1/2 PSD-95-PAGFP (that includes the 67 amino acid linker region between PDZ2 and 3) was amplified by PCR and subcloned at the sites EcoRI/KpnI in front of the first 64 amino acid of the N terminus of PSD-95 in frame in the PAGFP-N1 vector (Craven et al., 1999). To create the mutants of PSD-95 at S73, the Quickchange site-directed mutagenesis kit (Stratagene) was used according to manufacturer instructions. The cDNAs of PSD-95, S73A PSD95 and S73D PSD-95 and ΔGK PSD-95 were amplified by PCR and subcloned in the pCI vector (Promega) at the XhoI/KpnI sites. PAGFP SHANK2 was generated by PCR amplification of PAGFP and subcloned at the sites NheI/SalI in frame with SHANK2.

The levels of anchored PAGFP tagged PSD-95 in the spine were estimated from the green/red fluorescence (G/R) ratio immediately after photoactivation. Since the concentration of transfected dsRed was held constant and a uniformly sized population of

spines was analyzed, this ratio is proportional to the number of PAGFP tagged PSD-95 molecules in the spine head. By this metric, more ($P<0.05$) WT PSD-95 (G/R=0.77 ± 0.6) was found in the spine head than S73A (0.43 ± 0.05) and S73D (0.46 ± 0.04) PSD-95. Therefore the differences in spine growth, protein trafficking, and LTP between the S73A and S73D can not be attributed to differences in expression levels. Furthermore, the S73A mutant enhanced spine growth despite being present at lower levels in the spine than WT PSD-95. Similar analysis was performed for SHANK2-PAGFP G/R ratios revealing no significant differences when SHANK2-PAGFP was expressed alone (G/R=0.32 ± 0.09), with S73A PSD-95 (0.37 ± 0.09), or with S73D PSD-95 (0.58 ± 0.09). Levels of SHANK2-PAGFP were increased ($P<0.05$) by co-expression of PSD-95 WT (0.91 ± 0.10) or ΔGK mutant (1.10 ± 0.07). However, given that spine growth is normal in SHANK2-PAGFP/WT PSD-95 neurons and absent in SHANK2-PAGFP/ΔGK PSD-95 neurons, these higher expression levels are not correlated with the activity-dependent spine growth and SHANK2 trafficking phenotypes.

Choice of approach for analysis of LTP

Analysis of LTP magnitude in GFP transfected neurons was accomplished by delivering the plasticity-inducing stimulus (PS) to a single spine of a neuron that was not under electrical control. 15-20 minutes after the PS, a whole-cell voltage-clamp recording was obtained from the stimulated neuron and the size of uncaged-evoked excitatory postsynaptic currents (uEPSCs) at the stimulated spine and its unstimulated neighbors were measured. In order to minimize the number of trials necessary to accurately measure uEPSC amplitude and to be able to rapidly sample many spines, 1 ms uncaging pulses were used to probe each spine. In addition, 1 mM MK801 was included in the intracellular solution to minimize the NMDAR contribution to the uEPSC (Brasier and Feldman, 2008). If LTP had been induced at the PS-stimulated spine, we expect $uEPSC_{PS}$ to be on average larger than $uEPSC_{control}$. This approach was chosen for several reasons. First, it prevents the confound of the rapid and variable wash-out of LTP due to dialysis of the cytoplasm that occurs when the whole-cell recording is obtained prior to LTP induction. In our approach the PS is delivered to a neuron whose intracellular environment has not been perturbed. Second, it allows manipulation of the intracellular environment (i.e. introduction of Cs and MK801) during measurement of the uEPSC in

order to obtain higher quality voltage- and space-clamp(Williams and Mitchell, 2008). Third, there is no selection bias in the choice of the postsynaptic terminal to be analyzed beyond the basal morphology of the associated spine. In contrast, studies of EPSCs generated by electrical stimulation of axons are biased towards the analysis of strong, proximal, and high-probability of release synapses that dominate the compound EPSC or that are typically first identified in minimal stimulation studies.

Figure preparation

All quantification of fluorescence intensities was performed from raw fluorescence intensities as recorded by the microscope data acquisition device. Figures were prepared in Adobe Photoshop and Illustrator. For display purposes, for each PAGFP- and GFP-fusion protein, a linear grayscale was chosen and kept constant in all panels displaying neurons transfected with that fusion protein.

Lentivirus	AMPAR EPSC			NMDAR EPSC		
	Non-infected	Infected	Ratio	Non-infected	Infected	Ratio
shPSD95 WT PSD-95	-30.0 ± 3.1 pA	-70.9 ± 6.9 pA *	2.93 ± 0.42	40.7 ± 4.5 pA	55.3 ± 9.8 pA *	1.37 ± 0.14
shPSD95 S73A PSD-95	-22.0 ± 2.5 pA	-55.1 ± 4.7 pA *	3.13 ± 0.41	35.7 ± 5.0 pA	50.1 ± 4.7 pA *	1.62 ± 0.17
shPSD95 S73D PSD-95	-26.0 ± 3.0 pA	-68.2 ± 7.0 pA *	2.99 ± 0.28	57.5 ± 6.5 pA	64.8 ± 7.2 pA	1.16 ± 0.06

Sup Table 1. Effects on EPSCs of replacement of endogenous PSD-95 with WT PSD-95, S73A PSD-95, or S73D PSD-95.
This table gives the numbers represented graphically in Figure 4. Simultaneous, dual whole-cell recordings were established from an infected and closely adjacent uninfected cell (as indicated by GFP expression and lack thereof, respectively). AMPAR EPSCs were recording at -60 mV and stimulus strength was adjusted so that AMPAR EPSCs in control cells were 10-50 pA. 40-70 traces were averaged to obtain the basal AMPAR EPSCs from the two cells. AMPAR EPSC amplitudes were measured using a 2 ms window around the peak. Cells were depolarized to +40 mV, allowed to stabilize and another 25-50 dual component EPSCs were collected to obtain a measurement of NMDAR EPSCs. NMDAR EPSC amplitudes were measured 60-65 msec after the initiation of the EPSC. Comparisons between infected and uninfected cell responses were done using paired t-tests and * in the infected column significant differences ($p<0.05$).

Supplementary Figure Legends

Sup. Figure 1. Changes in spine head volume induced by 2 PLU of MNI-glutamate.
(A) Average time course of changes in spine volumes from neurons expressing dsRed and imaged to generate the data shown in Figure 1B. The red, black and blue circles represent data for stimulated spines, unstimulated spines and stimulated spines in presence of CPP as in Figure 1B, respectively. In the subsequent panels, * and # indicates $p<0.05$ for data at 11 minutes and for the average data between minutes 21-31.
(B) As in panel A for neurons expressing dsRed and either WT PSD-95 (red circle) or shPSD-95 (blue circle). Spines were imaged to generate the data shown in Figure 1F. For comparison, the data corresponding to stimulated spines from dsRed-positive neurons from Sup. Figure 1A are replotted in the gray shaded regions (mean ± SEM).
(C-D) As in panels A and B. The red circles are calculated from experiments shown in Figure 2B and 2C from neurons expressing either dsRed (C) or dsRed and WT PSD-95 (D) in the presence of KN-93. For comparison, the data from spines overexpressing dsRed (C) or dsRed and WT PSD-95 (D) untreated are replotted in the gray shaded area.
(E-J) As in panels A-D. The red circles correspond to dsRed and either S73A PSD-95 (E), S73D PSD-95 (F), ΔPDZ1,2 PSD-95-GFP (G), ΔGK PSD-95-GFP (H), S73A-ΔGK PSD-95-GFP **(I)**, or S73D-ΔGK PSD-95-GFP (J) expressing neurons from, respectively, Figure 2E, 2F, 6E, 6F, 6G, and 6H. The gray shaded area represents the data from WT PSD-95 replotted for comparison.
(K) As in panels A-J, for neurons expressing dsRed and PAGFP-SHANK2 (red circle) from Figure 7E. For comparison the gray shaded area is the data from neurons expressing dsRed.

Sup. Figure 2. PS-induced spine growth is stable for a period of time of at least 3h.
(A) Representative images spines from a neuron expressing dsRed and shPSD-95-WTPSD-95-GFP. The indicated spine was stimulated with PS (t=10 min, arrowhead).
(B) Average time course of spine head cross-sectional area of neurons expressing dsRed and shPSD-95-WTPSD-95-GFP (blue circles, n = 8/3 spines/cells). For comparison, data

(mean +/- SEM) from panel (B) for dsRed-only expressing neurons are replotted in the gray shaded region.

(C) As in panel A for spines from a neuron expressing dsRed. The indicated spine was stimulated with PS (t=10 min, arrowhead). Images were acquired every 5 min during the first 30 min and then every 30 minutes during 3h.

(D) As in panel B for spines from neurons expressing dsRed (red circles, n = 6/6 spines/cells). The gray shaded area is the data from the time course of neurons expressing dsRed from Figure 1B.

Sup. Figure 3. Fluorescence of PAGFP-PSD-95 within individual spine heads reports its release from a tethered pool in the spine as well as changes in the size of this pool over time.

(A) Representative image of a spine expressing PSD-95-PAGFP that was exposed to 2 photoactivating pulses (PA1 and PA2) separated by 1 minute. No additional photoactivation is achieved with the second pulse, indicating that all fluorophores were activated by the initial pulse.

(B) Ratio of the green fluorescence in the spine after the 2^{nd} photoactivation pulse relative to that after the 1^{st} (n = 23/4 spines/cells).

(C) Time-course of PSD-95-PAGFP in photoactivated spines imaged every 5 min (black circles, n = 45/9 spines/cells) or every 15 min (gray triangles, n = 32/9 spine/cells).

Sup. Figure 4. Spines subjected to plasticity-inducing stimulus from neurons expressing WT PSD-95 are of the same size as those from neurons expressing dsRed alone.

(A) Prestimulated apparent spine head width (*left*) or length (*right*) (see methods) from neurons expressing either dsRed (black bar, n = 22/4 spines/cells) or dsRed and WT PSD-95 (red bar, n = 30/8 spines/cells) used to generate the data in Figure 1. Larger spines resulting from overexpression of PSD-95 can also be identified (blue bar n = 16/6 spines/cells) but were not chosen for analysis beyond this figure. Error bars represent SEM.

(B) Representative images of stimulated spines from neurons expressing dsRed and WT PSD-95. Images represent example of normal sized (*top*) or large (*bottom*) spines resulting from the overexpression of PSD-95.

(C) Average time course of spine area of stimulated spines from neurons expressing dsRed and WT PSD-95 (normal spine size, red circles, n = 30/8 spines/cells; large spine size, blue circles, n = 16/6 spines/cells). For comparison, the data for spines from neurons expressing dsRed alone re replotted in the gray area

Sup. Figure 5. Repetitive 2PLU of MNI-glutamate with 810 nm laser light does not induce spine head enlargement.

(A) Average time course of spine head area of stimulated spines from neurons expressing dsRed (red circle, n = 8/3 spines/cells) stimulated by PS using 810 nm laser light. The data of stimulated spines from dsRed expressing neurons using 720 nm laser light is replotted in the gray shaded area. Red open circles represent statistic difference of $P<0.05$ when comparing 810 nm and 720 nm stimulated spines.

Sup. Figure 6. KN-93 does not affect the basal stability of PSD-95-PAGFP but impaired its transient removal from spine head induced by PS.

(A) Representative images and time-courses of PSD-95-PAGFP fluorescence in dendritic spines of neurons either as control (images from Figure 2A) *(top)* or in the presence of 10 μM KN-92 *(middle)* or 10 μM KN-93 *(down)*.

(B) As in panel (A) for spines receiving PS (t=0, arrowhead) and preincubated with 10 μM KN-93

(C) Average time-course of PSD-95-PAGFP fluorescence in spines of slices that were preincubated with either KN-92 (black, n = 29/11 spines/cell) or KN-93 (red, n=25/6 and 59/13 spines/cells). The shaded gray region shows behavior of PSD-95-PAGFP in absence of treatment.

(D) As in panel C for spines receiving PS and treated with 10 μM KN-93 (red, n=10/4 spines/cells). For comparison the pink and gray shaded area representing data from non simulated or stimulated spines from neurons expressing WT PSD-95 are replotted.

(E) Average time course of spine head area of stimulated spines from neurons expressing dsRed and WT PSD-95 (red, n=10/4 spines/cells) and preincubated with 10 μM KN-93. The gray shaded area corresponds to data from stimulated spines overexpressing WT PSD-95 in absence of KN-93. # symbol indicates statistical significant differences ($P<0.05$) compared to the data in the gray region at between minutes 21-31.

Sup. Figure 7. KN-93 impairs the persistent spine growth in spines of neurons expressing S73A PSD-95.

(A) Representative images of spines form neurons expressing dsRed and S73A PSD-95 in the presence of 10 μM KN-93. Spine were photoactivated (white box, t = 0 min, PA) with 810 nm laser light and stimulated with PS (t=10 min, arrowhead). The same spine was subjected to a second photoactivation pulse (PA') at the end of the imaging period.

(B) Average time course of S73A PSD-95-PAGFP fluorescence in spines receiving PS of slices that were preincubated with KN-93 (red, n = 13/4 spines/cells). The pink and gray shaded area represent data from, respectively, unstimulated or stimulated spines expressing dsRed and S37A PSD-95 and are replotted for comparison.

(C) Average time course of spine head area of stimulated spines from neurons expressing dsRed and S73A PSD-95 (red, n = 10/4 spines/cells) and preincubated with 10 μM KN-93. The gray shaded area corresponds to data from stimulated spines overexpressing WT PSD-95 in absence of KN-93. # symbol indicates statistical significant differences ($P<0.05$) compared to the data in the gray region at between minutes 21-31.

Sup. Figure 8. Spines from neurons expressing dsRed and SHANK2 selected for plasticity-induced stimulus are the same size as those selected from neurons expressing dsRed

(A) Prestimulated apparent spine head width (*left*) or length (*right*) (see methods) from neurons expressing either dsRed (black, n = 22/4 spines/cells) from Figure 1A, B or dsRed and PAGFP-SHANK2 (red, n = 19/3 spines/cells) that were imaged to generate data of Figure 8D. Large spines due to ovexpression of PSD-95 could also be identified (blue bar n = 7/3 spines/cells) but were not analyzed further beyond what is shown inthis figure. Error bars represent SEM.

(B) Images of a stimulated large spine (arrowhead) from neurons expressing dsRed and PAGFP-SHANK2. A normal sized spine is seen in the lower portion of the image for comparison.

(C) Average time course of spine area of stimulated large spines from neurons expressing dsRed and PAGFP-SHANK2 (red, n = 7/3 spines/cells). For comparison, the data for normal sized spines from neurons expressing PAGFP-SHANK2 are replotted in the gray area.

Sup. Figure 9. The basal stability of PAGFP-SHANK2 is not affected by expression of ΔGK PSD-95, S73A PSD-95, or S73D PSD-95

Average time course of PAGFP-SHANK2 fluorescence in spines from neurons expressing dsRed, PAGFP-SHANK2, and either WT PSD-95 (black, n = 15/5 spines/cells), ΔGK-PSD-95 (red, n = 27/5 spines/cells), S73A PSD-95 (green, n = 20/5 spines/cells), or S73D PSD-95 (blue, n = 11/3 spines/cells) after photoactivation. Error bars represent SEM.

Sup. Figure 10. Inhibition of activity-dependent spine growth in neurons expressing GFP-SHANK2 and ΔGK PSD-95

(**A**) Time-lapse images of spines expressing dsRed, ΔGK PSD-95, and GFP-SHANK2. The indicated spine received PS (t=10 min, arrowhead).

(**B**) Average time course of GFP-SHANK2 fluorescence in spines of cells expressing ΔGK PSD-95 that received PS (red, n = 12/3 spines/cells). The gray shaded area shows the behavior of SHANK-GFP (mean ± SEM) in stimulated spines expressing only dsRed and symbols designate $p<0.05$ compared to this data at t=11 min (*) or for the average data between minutes 21-31 (#).

(**C**) Average time course of spine head cross-sectional area of stimulated spines from neurons expressing GFP-SHANK2, ΔGK PSD-95 and dsRed (red, n = 12/3 spines/cells) that were imaged to produce the data shown in Figure 8E, F. The gray shaded area (mean ± SEM) corresponds to spines that express GFP-SHANK2 and dsRed from Figure 7D. Symbols designate $p<0.05$ compared to this data at t=11 min (*) or for the average data between minutes 21-31 (#).

Sup. Figure 11. Regulation of PSD-95 serine 73 controls the activity-dependent translocation of SHANK2 out of spine head.

(A) Representative images of spines from neurons expressing dsRed and either S73A PSD-95-PAGFP (*top*) or S73D PSD-95-PAGFP (*bottom*). PAGFP in a single spine was photoactivated (white box, t = 0 min) and changes in fluorescence intensity were monitored by time-lapse imaging. The same spine was subjected to a second photoactivation pulse (PA') at the end of the imaging period.

(B) Average time course of PAGFP fluorescence from spines expressing PAGFP-SHANK2 and S73A PSD-95 after photoactivation and PS (red, n = 13/4 spines/cells). The gray shaded area represents the PAGFP-SHANK2 fluorescence (mean ± SEM) of stimulated spines from neurons esxpressing PAGFP-SHANK2 alone replotted for comparison. Open red circles indicate statistically significant differences ($P<0.05$) between stimulated and unstimulated spines.

(C) Average time-course of stimulated spine areas from neurons expressing dsRed, PAGFP-SHANK2 and S73A PSD-95 (red circles, n = 13/4 spines/cells). The gray shaded area (mean +/- SEM) corresponds to data for spines expressing dsRed and PAGFP-SHANK2 and symbols represent statistically significant differences ($P<0.05$) with this data at minute 11 (*) or for the average between minutes 21 to 31 (#).

(D) As in panel B for spines from neurons expressing dsRed, PAGFP-SHANK2 and S73D PSD-95 (red circles, n = 7/3 spines/cells)

(E) As in panel C for spines from neurons expressing dsRed, PAGFP-SHANK2 and S73D PSD-95 (red circles, n = 7/3 spines/cells)

SUPPLEMENTARY 1

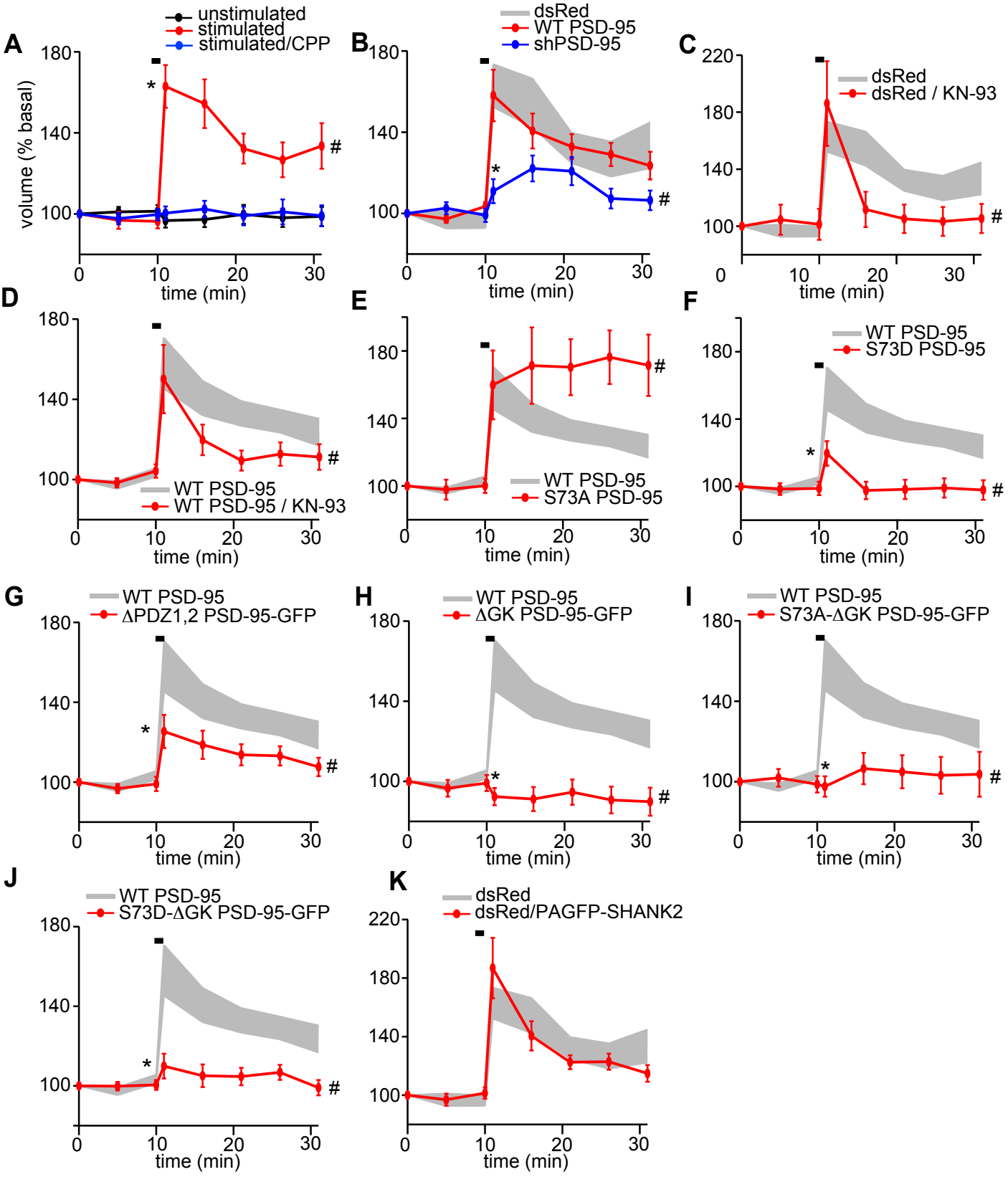

SUPPLEMENTARY 2

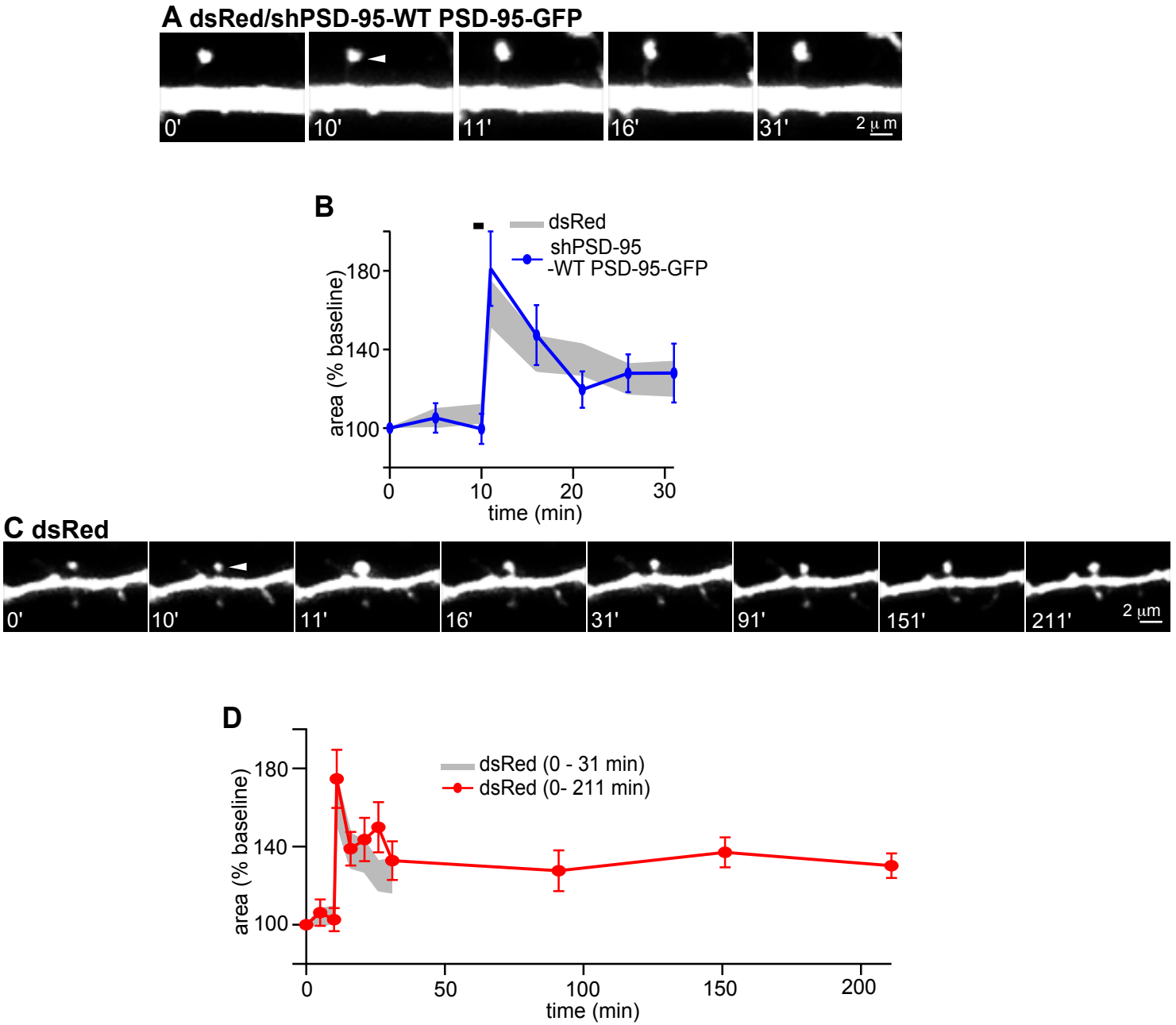

SUPPLEMENTARY 3

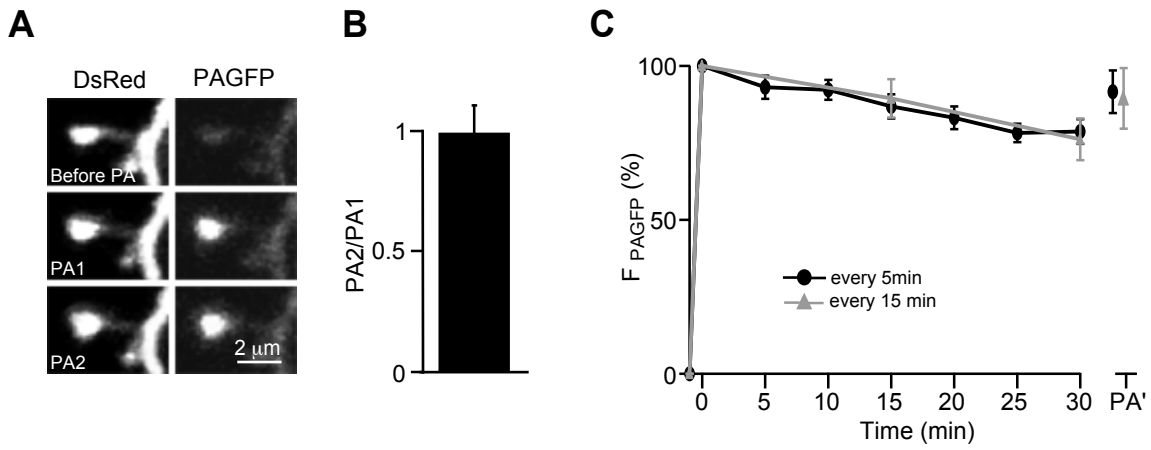

SUPPLEMENTARY 4

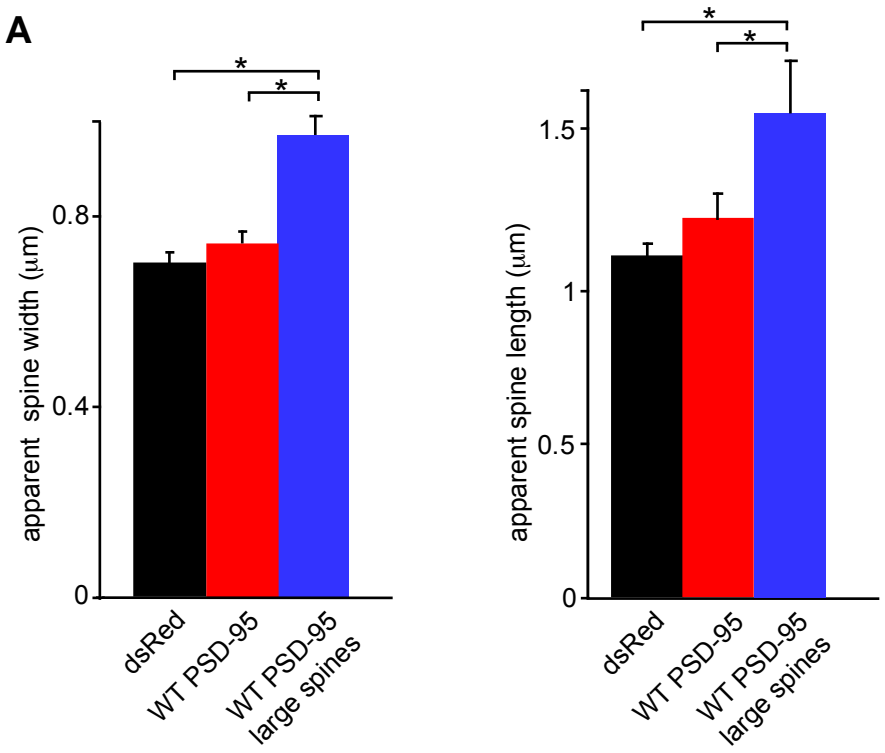

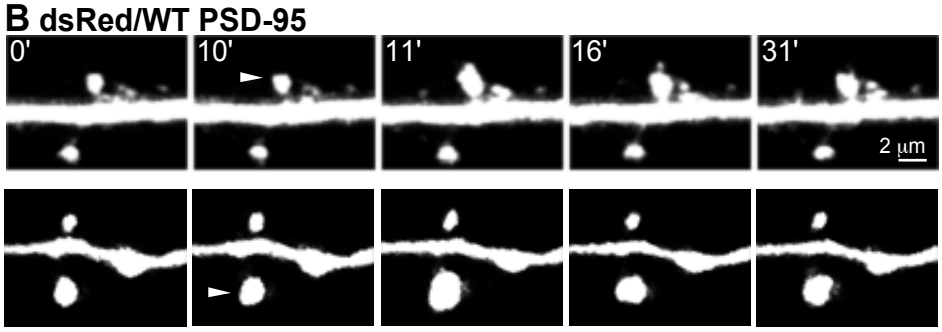

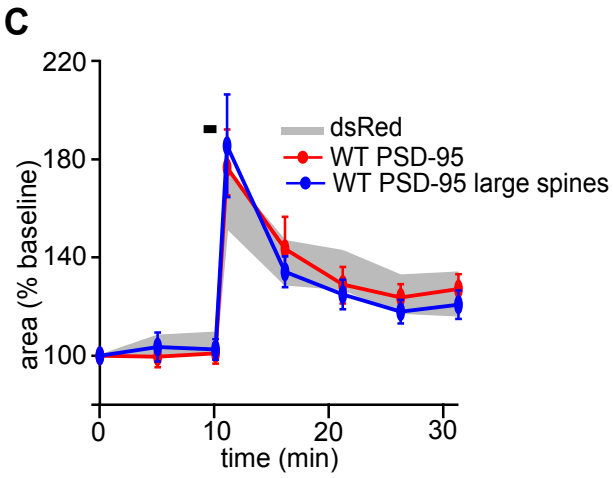

SUPPLEMENTARY 5

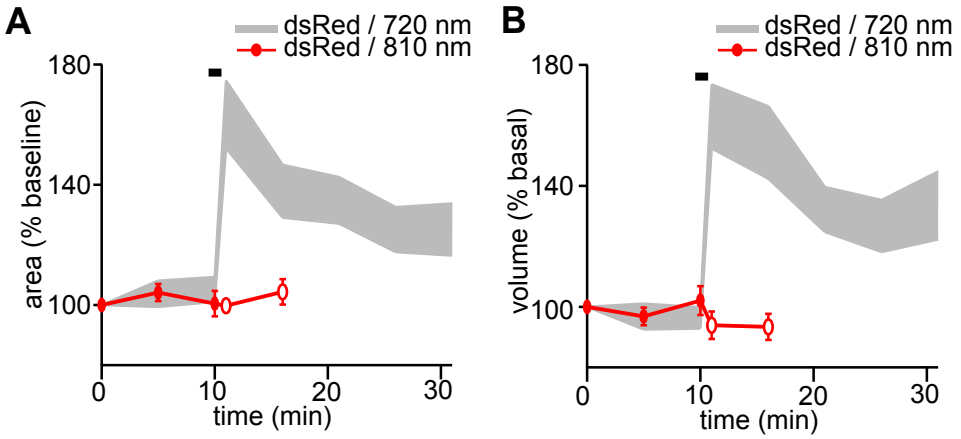

SUPPLEMENTARY 6

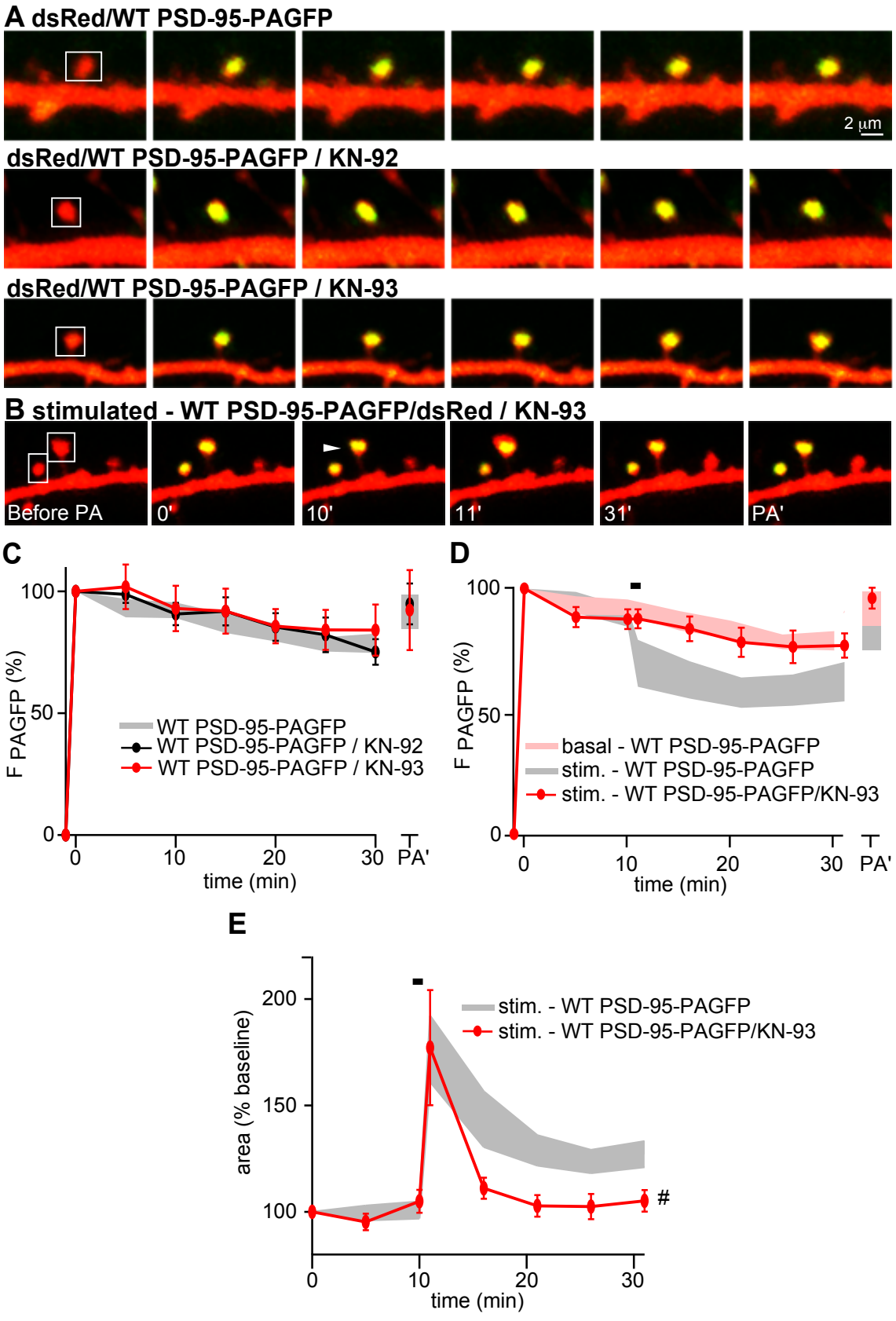

SUPPLEMENTARY 7

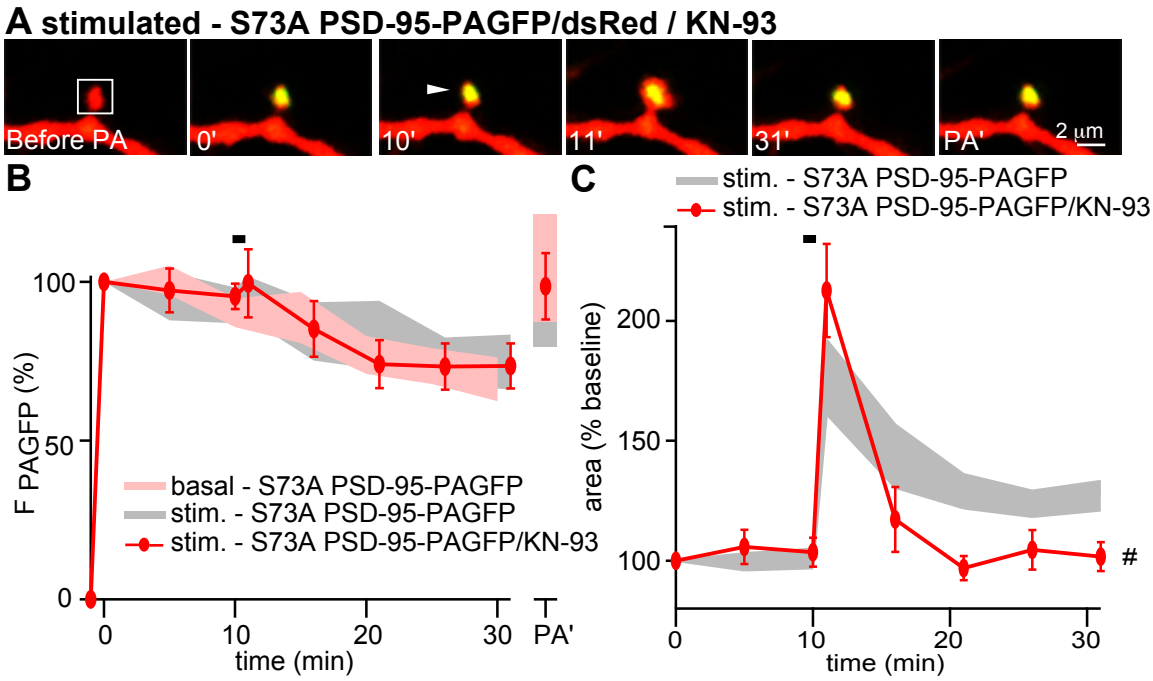

SUPPLEMENTARY 8

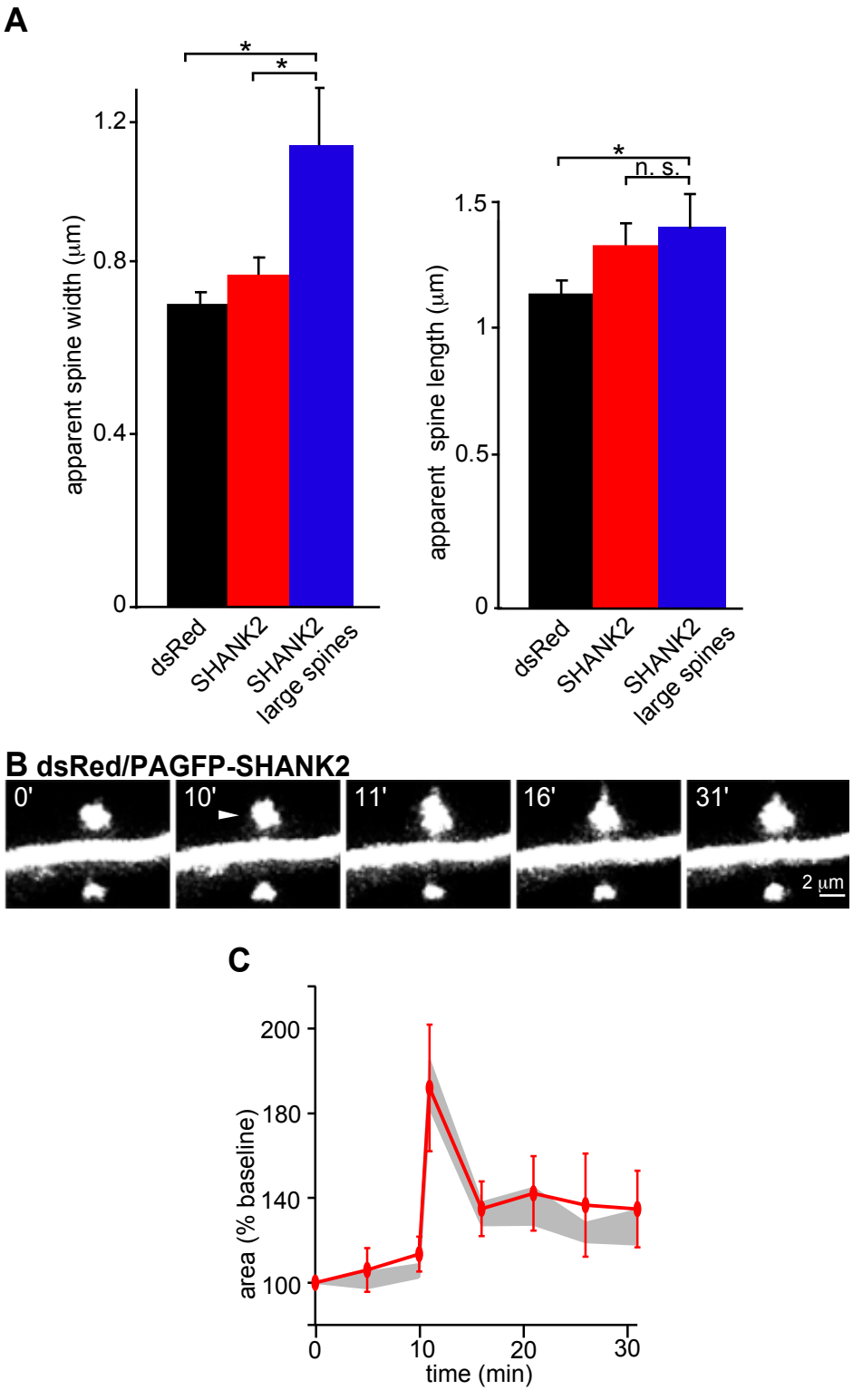

SUPPLEMENTARY 9

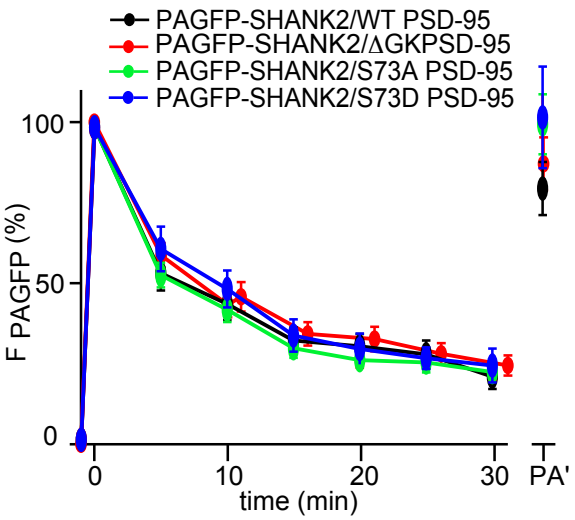

SUPPLEMENTARY 10

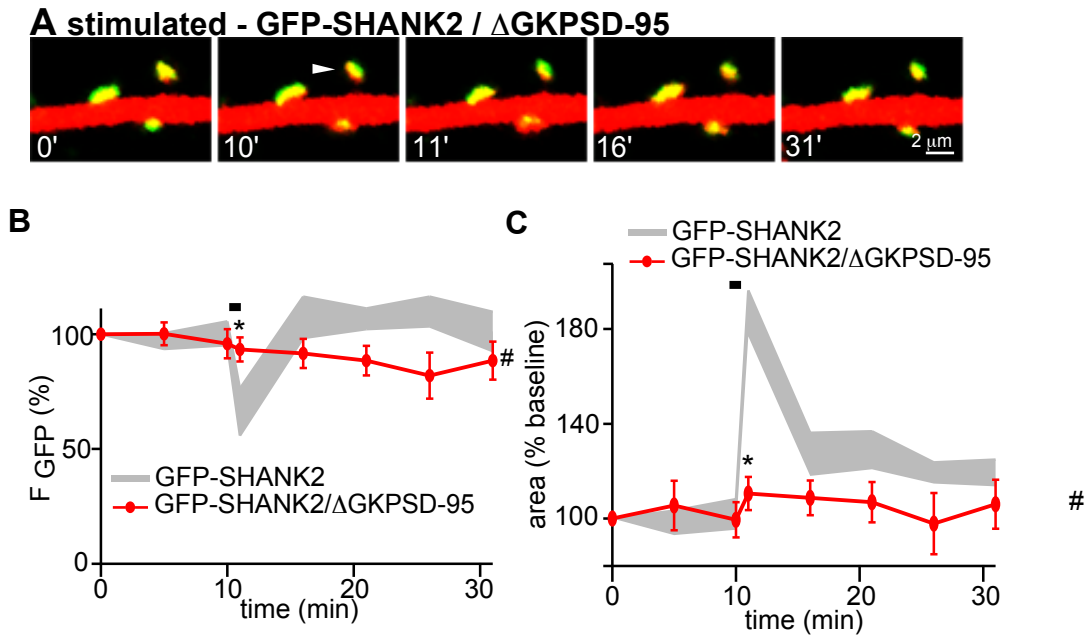

SUPPLEMENTARY 11